

***Final Draft***  
of the original manuscript:

Homaeigohar, S.; Dai, T.; Elbahri, M.:

**Biofunctionalized nanofibrous membranes as super separators of protein and enzyme from water**

In: Journal of Colloid and Interface Science (2013) Elsevier

DOI: 10.1016/j.jcis.2013.05.076

# **Biofunctionalized nanofibrous membranes as super separators of Protein and Enzyme from Water**

**Shahin Homaeigohar<sup>a</sup>, Tianhe Dai<sup>a</sup>, and Mady  
Elbahri<sup>a,b,\*</sup>**

a: Helmholtz-Zentrum Geesthacht, Institute of Polymer Research, Nanochemistry and  
Nanoengineering group, Max-Planck-Str. 1, 21502 Geesthacht, Germany

b: Nanochemistry and Nanoengineering group, Institute for Materials Science, Faculty of  
Engineering, University of Kiel, Kaiserstrasse 2, 24143 Kiel, Germany

## **Abstract**

Here, we report development of a novel biofunctionalized nanofibrous membrane which despite its macroporous structure, it is able to separate even trace amounts (as low as 2 mg/L) of biomolecules such as protein and enzyme from water with an optimum efficiency of ~90%. Such an extraordinary protein selectivity at this level of pollutant concentration has never been reported. In the current study, poly(acrylonitrile-co-glycidyl methacrylate) (PANGMA) electrospun nanofibers are functionalized by a bovine serum albumin (BSA) protein. This membrane is extraordinarily successful in removal of BSA protein and *Candida Antarctica* Lipase-B (Cal-B) enzyme from a water based solution. Despite a negligible non-specific adsorption of both BSA and Cal-B to the PANGMA nanofibrous membrane (8%), the separation efficiency of the biofunctionalized membrane for BSA and Cal-B reaches to 88% and 81%, respectively. The optimum separation efficiency at a trace amount of protein models is due to the water-induced conformational change of the biofunctional agent. The conformational change not only exposes more functional groups available to catch the biomolecules but also leads to swelling of the nanofibers thereby a higher steric hindrance for the solutes. Besides the optimum selectivity, the biofunctionalized membranes are wettable and mechanically stable thereby highly water permeable.

**Keywords:** Electrospinning, nanofibrous membrane, biofunctionalization, protein separation, water filtration

## ▪ Introduction

Water shortage all around the world is becoming a global crisis threatening the human kind's life. One main reason for such a crisis is certainly the water pollution. Accordingly, water purification seems to be the basic solution. Of the most important pollutants, water quality is highly sensitive to the organic ones. Such organics even at a very low concentration e.g. no more than 1% of the pollution in a river, are able to use up the dissolved oxygen, making the water free of any life. <sup>1</sup>

Membranes such as micro-, ultra- and nanofiltration ones are frequently used for remediation of wastewaters. The principal separation function is based on sieving mechanism i.e. needing to a pore with a dimension smaller than the solute size. For very small solutes, the pore size is so small that it necessitates applying a high pressure drop and huge energy consumption for the filtration process.

In contrary to the normal sieving based membranes, functionalized membranes have been developed to allow the separation of molecules based on physical/chemical properties or biological functions rather than molecular weight/size. This interaction based separation circumvents any need to design of very small pore sizes thereby huge feed pressures. Indeed a functionalized membrane whose surface is equipped to immobilized specific ligands, separate or capture molecules selectively.<sup>2</sup> Other than filtration applications, such kind of membranes are desired for biotechnology industry as affinity membrane chromatography to purify proteins and other biomolecules from biological fluids as well. <sup>2</sup>

Electrospun nanofibrous membranes (ENMs) are a novel class of membranes to be used for water filtration. A high interconnected porosity and huge surface area make

them an attractive candidate for the class of functionalized membranes. While the first property gives rise to an extraordinary permeability thereby a very low energy consumption, the latter one leads to the feasibility of a high amount of functionalization required for extraordinarily selective membrane applications. Accordingly, the biofunctionalized polyurethane, polysulfone, polyacrylonitrile and cellulose nanofibrous membranes have been examined for protein and enzyme (e.g. IgG, BSA, lipase, bromelain etc.) separations.<sup>2-5</sup> Despite an optimum potential expected for protein selectivity, most of this group of membranes when using a protein solution with a few mg/mL concentration could show a low adsorption capacity mainly around 10% equal to 13-41 mg/g nanofibrous membrane.<sup>2, 6, 7</sup> Noteworthy, the protein adsorption tests have been performed in a static (batch) mode i.e. immersion of the membrane in the solution for a given time i.e. the chance of adsorption of the protein increases in such a manner. Besides a low to moderate protein selectivity, the preparation process of the mentioned functionalized membranes including electrospinning, surface modification and functionalization seems to be challenging. For example, electrospinning of cellulose has been reported to be complicated<sup>2</sup> or surface modification of polysulfone involving plasma treatment and subsequent grafting does not seem a very simple and straightforward approach.<sup>8</sup>

In the forthcoming study, we aim to introduce a biofunctionalized nanofibrous membrane with an extraordinarily higher separation efficiency for biomolecules and fabricated in a simpler manner than its already established counter parts. The biomolecule selectivity of this membrane will be evaluated in the most challenging conditions compared to the previously performed studies. First, a protein solution model with a trace

concentration (in the scale of mg/L instead of mg/mL used by the other researchers<sup>2, 4-6</sup>) is employed. This solution is assumed to pass easily through a macroporous nanofibrous membrane. Second, the filtration will be performed in a dynamic filtration mode which minimizes the residence time of protein on the nanofibers and lowers the chance of adsorption of the protein. A high protein separation efficiency if obtained proves the extraordinary selectivity of our biofunctionalized membrane.

Recently, we could show a biofunctionalization concept highly efficient in term of selective removal of water pollutants e.g. metal nanoparticles.<sup>9</sup> In our belief, this approach could be also applicable for selective removal of biomolecules such as proteins and enzymes with a high efficiency. Thus, here, we aim to prove that a protein (e.g. BSA) functionalized poly(acrylonitrile-co-glycidyl methacrylate) (PANGMA) nanofibrous membrane through functionality and conformational change of the biofunctional agent could optimally separate biomolecule pollutants from waste water streams.

As the biofunctional agent, BSA is a cheap serum albumin protein, widely used in numerous biochemical applications. The nanofibrous substrate is made of PANGMA which is a new copolymer of acrylonitrile (AN) and glycidyl methacrylate (GMA).<sup>10</sup> The strong backbone of the polymer composed of polyacrylonitrile confers a suitable chemical stability, while the presence of a free and active epoxy group on GMA could lead to its high functionality. Thus, the nanofibers could be readily functionalized via the reaction between the amine and epoxy groups of BSA and PANGMA, respectively.<sup>10, 11</sup> In the forthcoming study, the filtration efficiency of the BSA/PANGMA ENMs in removal of two protein models from their highly dilute aqueous solutions is investigated.

Probable influences of the biofunctionalization on structural properties including thermal and mechanical properties, wettability, pore size and porosity will also be characterized.

## ▪ **Experimental section**

**Materials.** Poly(acrylonitrile-co-glycidyl methacrylate) (PANGMA) was synthesized at Helmholtz-Zentrum Geesthacht (HZG) (Previously GKSS Forschungszentrum GmbH)<sup>12</sup> with a molecular weight ( $M_n$ ) of ca. 100,000 g/mol and GMA content of 13 mol%. Bovine Serum Albumin (BSA) (dried powder) and Phosphate Buffered Saline (PBS) were purchased from Sigma-Aldrich Co. *Candida antarctica* lipase B (Cal-B) (dried powder) and *N,N*-dimethylformamide (DMF) were purchased from Merck KGaA and BioCatalytics Co. (Grambach, Austria), respectively. All the chemicals were directly used without purification.

**Electrospinning of PANGMA nanofibers.** *N,N*-dimethylformamide (DMF) was used to dissolve PANGMA (20 wt%). The solution was fed with a constant rate of 1.1 mL/h into a needle by using a syringe pump (Harvard Apparatus, USA). The electrospinning was done on an Aluminum (Al) foil located 25 cm above the needle tip for 4 h by applying a voltage of 15-20 kV (Heinzinger Electronic GmbH, Germany). After all, the nanofibrous mat was peeled off from Al foil and dried under vacuum at 30 °C for 24 h to remove the residual solvent.

**Biofunctionalization of PANGMA nanofibers.** The PANGMA nanofibrous mats were immersed into the BSA/PBS buffer (5 mg/mL) (pH 6.8) while gently shaken at 55 °C for 24 h. Subsequently, to remove all the unbound BSA, the membranes were

taken out and washed several times by PBS buffer (pH 6.8) then de-ionized water and dried under vacuum at 30 °C for 24 h.

The morphology of the PANGMA ENMs as neat and biofunctionalized was observed with a scanning electron microscope (LEO Gemini 1550 VP, Zeiss) at 10 kV accelerating voltage after gold-coating. The diameter of the electrospun nanofibers was determined from the SEM images using the Adobe Acrobat v.07 software.

Chemical surface analysis of both the neat and BSA immobilized PANGMA ENMs was performed by Fourier Transform Infra Red Spectrometry (FTIR). Attenuated total reflection Fourier transform infrared (ATR-FTIR) spectra were recorded using a Bruker Equinox 55 spectrometer.

**Protein (ligand) leaching test.** The amount of leaching of the immobilized BSA was characterized by a so-called leaching test. A custom-made water circulating set-up (Figure 1) consisting of a membrane module, a pump and a reservoir was utilized for the test. The reservoir was filled with 500 mL deionized water circulated by the pump within the set-up and passing through the membrane for up to 168 h.

The BSA leaching was characterized by measuring the amount of the dissociated BSA from the membranes present in the water flow (equation (1)):

$$L = \frac{(W_0 - W_t)}{W_0} \times 100\% = \frac{W_{dt}}{W_0} \times 100\% \quad (1)$$

where L is the BSA leaching value (wt%),  $W_0$  (mg) and  $W_t$  (mg) are the initial and momentary amount of the bound BSA on the PANGMA ENM, respectively thereby  $W_{dt}$  (mg) is the momentary amount of the dissociated BSA present in water.



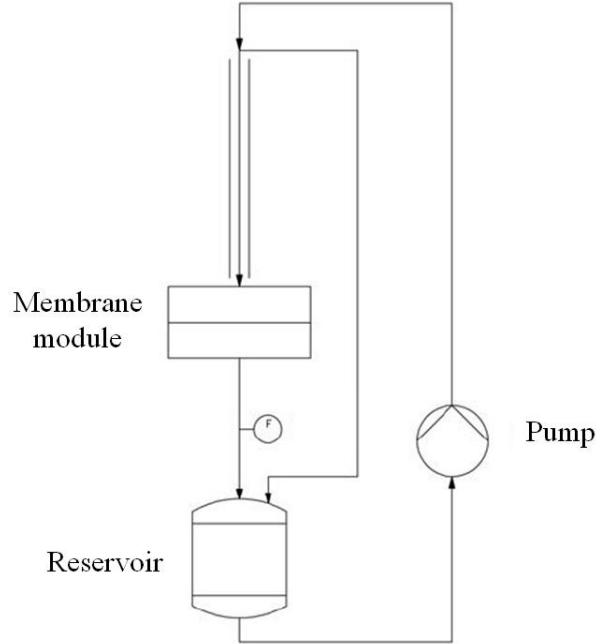


Figure 1 Schematic of the set-up used for the leaching test

**Pore size and porosity measurement.** As biofunctionalization could lead to alteration of structural characteristics of the PANGMA nanofibrous membranes, pore size and porosity of the membranes before and after functionalization were measured. The porosity of the PANGMA ENMs was calculated according to the equation (2)<sup>13</sup>:

$$\varepsilon = 1 - \frac{\rho}{\rho_0} \times 100\% \quad (2)$$

where  $\varepsilon$  is porosity,  $\rho_0$  and  $\rho$  are the bulk density of PANGMA and apparent density of the PANGMA electrospun mat, respectively. To measure the apparent density, thickness of the mats with known area and mass (already measured by an electronic balance with a resolution of 0.1 mg) was determined by using a digital micrometer (Deltascop® MP2C from Fischer).

The pore size of the PANGMA ENMs was characterized through a liquid-gas displacement method so-called “bubble point” test based on the measurement of the pressure necessary to blow a gas through a liquid-filled membrane pore. More details of this characterization can be found at <sup>14</sup>.

### **Wettability and Water uptake measurement of the BSA/PANGMA**

**nanofibrous membrane.** Wettability of the PANGMA ENMs was characterized through water contact angle measurement, using a contact angle analysis system (Krüss DSA 100, Germany). A 5 µl droplet was dispensed on the membrane and the resultant angle was measured.

Moreover, the water uptake capacity of the neat and biofunctionalized PANGMA ENMs was evaluated by their immersion in a water bath for up to 80 h and measuring the wet sample weight at different intervals. The water uptake capacity of the membranes was calculated according to the equation (3):

$$WU = \frac{(W_{wet} - W_{dry})}{W_{dry}} \times 100\% \quad (3)$$

Where  $W_{wet}$  and  $W_{dry}$  are the weight of the membranes in dry and wet states, respectively.

### **Evaluation of thermal properties of the BSA/PANGMA nanofibrous**

**membranes.** The probable influence of the biofunctionalization on thermal properties of the membranes was probed via DSC and TGA measurements.

DSC was performed by a Netzsch DSC 204 Phoenix® using indium standards. The glass transition temperature ( $T_g$ ) was determined by means of a dynamic scan at 10 °C/min from 20 to 300 °C.

The thermal stability of the neat and biofunctionalized ENMs was evaluated by TGA. Thermal gravimetric analysis (TGA) of the ENMs was carried out with a thermogravimetric analyzer of Netzsch 209 TG. TGA analysis was performed at 20–700 °C with a heating rate of 10 °C /min under Argon. The decomposition temperature ( $T_d$ ) was defined as the temperature at 5% weight loss.

**Evaluation of mechanical properties of the BSA/PANGMA nanofibrous membranes.** The biofunctionalized ENMs were characterized in term of mechanical properties by a tensile machine (Zwick/Roell Z020-20KN, Germany) equipped with a 20-N load-cell at ambient temperature. The cross-head speed was 2 mm/min and the gauge length was 20 mm. The reported tensile moduli and tensile strengths represent average results of 10 tests.

**Water flux measurements.** To assess the water permeability of the PANGMA ENMs as neat and functionalized, a water flux measurement was performed. To do so, the circular membranes ( $d=20$  mm) were stamped out and placed over a poly(*p*-phenylene sulfide) (PPS) technical nonwoven support layer. The hybrid membranes were subsequently put in the membrane module of a custom-built set-up (shown in <sup>15</sup>) and 300 mL water was passed through them under a 1 bar applied pressure. The water flux was calculated by equation (4):

$$J = \frac{Q}{A \cdot \Delta t} \quad (4)$$

where  $J$  is the water flux ( $L/h \cdot m^2$ ),  $Q$  is the permeated volume of water (L),  $A$  is the effective area of the ENMs ( $m^2$ ), and  $\Delta t$  is the sampling time (h). All the flux measurements were repeated three times.

**Protein filtration experiments.** The ability of the biofunctionalized ENMs in removal of proteins from water was investigated via a filtration experiment of two model proteins including BSA and Cal-B. The latter is in fact an enzyme able to act as a catalyst. Decoration of the nanofibers by the enzyme rejected during the filtration could lead to creation of a catalysis membrane or a membrane bioreactor (MBR).

To run the experiment, the membranes with an active filtration area of 2 cm<sup>2</sup> were placed in the membrane module of a custom-built set-up (Figure 2) and 20 mL protein aqueous solution (2 mg/L) was passed through them. Such a low protein concentration would challenge the filtration ability of our biofunctionalized ENM. A normal ENM with a macroporous structure is hardly able to catch trace amounts of water soluble pollutants. The driving force for the filtration was a minor hydrostatic pressure of 20 mPa supplied by the installed column on the module. The experiment was performed in a cyclic style i.e. every permeate was considered as the new feed for the new filtration cycle until completion of 5 successive cycles. Unlike the batch adsorption tests adopted in the similar studies, this dynamic mode of filtration minimizes the residence time of protein solutes on the nanofibers and strictly examines the selectivity of our membranes.

Already constructed the standard protein calibration curve, the concentration of the proteins in the original feed and permeates was specified by a UV-Vis spectroscopy. The filtration efficiency (FE) was determined according to the equation (5):

$$FE = \left(1 - \frac{C_p}{C_f}\right) \times 100\% \quad (5)$$

where  $C_p$  and  $C_f$  are the concentration of protein in the permeates and feeds, respectively.

## ▪ **Results and discussion**

**Morphological features of the biofunctionalized nanofibers.** The morphology of the nanofibers as neat and biofunctionalized is observed in Figure 3. As seen in the SEM images, no pore clogging occurs and the porosity remains unchanged. These qualities will be quantitatively discussed in a next section. As proved by measurement of the nanofiber diameters before and after biofunctionalization, immobilization of the BSA protein onto the nanofibers does not lead to a significant growth of their thickness (Figure 4). This behaviour can be interpreted as a uniform distribution of the protein immobilized along the nanofibers' body.

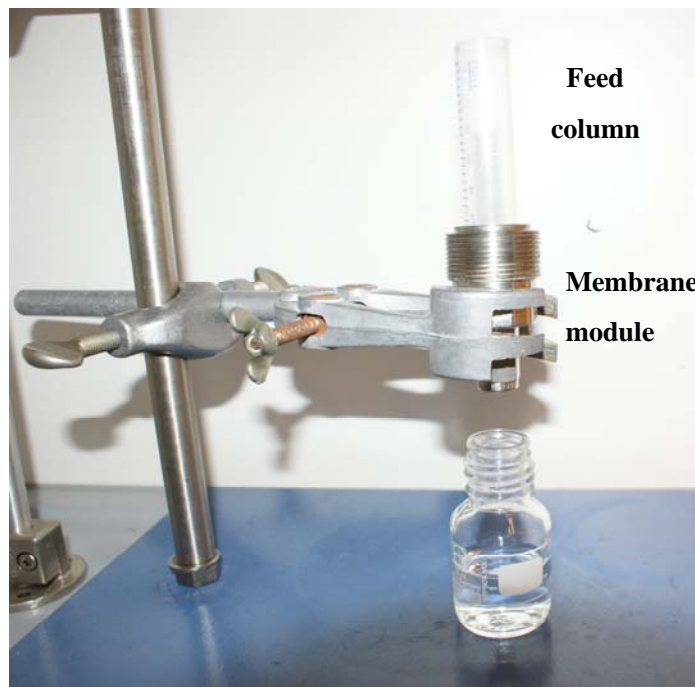


Figure 2 Schematic of the set-up used for the filtration test

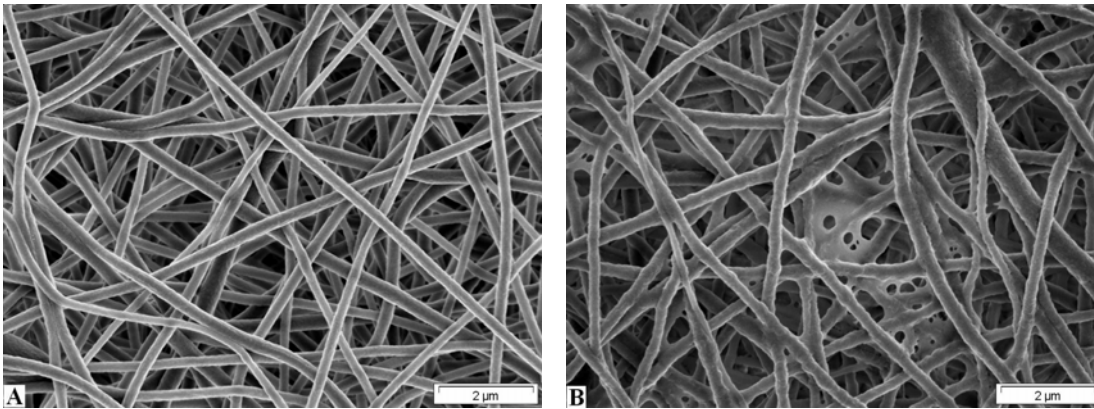


Figure 3 SEM micrographs showing the morphology of the nanofibrous membranes before (A) and after (B) biofunctionalization

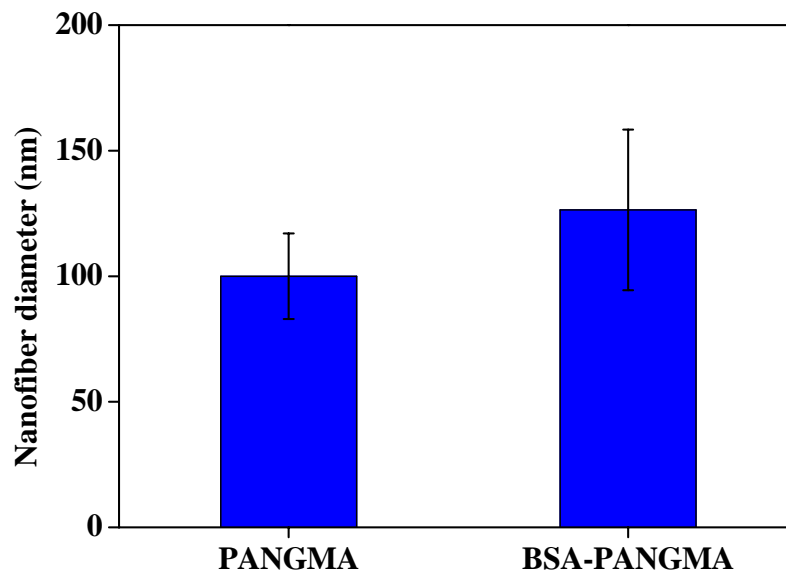


Figure 4 Average diameter of the PANGMA nanofibers as neat and BSA biofunctionalized

**Protein (ligand) leaching test.** To investigate how stable is the bonding between BSA ligands and PANGMA nanofibers, a leaching test was performed. As shown in Figure 5, despite a long time of 168 h continuously washing the membranes, the amount of the BSA leached is less than 1.2 wt%. In fact, this value represents the amount of the

physically adsorbed BSA which could be released during the test and under a more harsh conditions than simple washing with PBS. The result confirms a stable covalent bond between the protein and the nanofibers i.e. an efficient functionalization process. The chemical covalent bond could be easily tracked via ATR-FTIR. As shown in Figure 6, successful reaction between the amine groups of BSA and epoxides of PANGMA is deduced by vanishing the characteristic peak of epoxy group appearing at  $908\text{ cm}^{-1}$  for the neat nanofibers. In addition, the peaks emerging at  $1650\text{ cm}^{-1}$  and  $1530\text{ cm}^{-1}$  for the biofunctionalized nanofibers are the vibration peaks of amide I and amide II groups in BSA molecules.

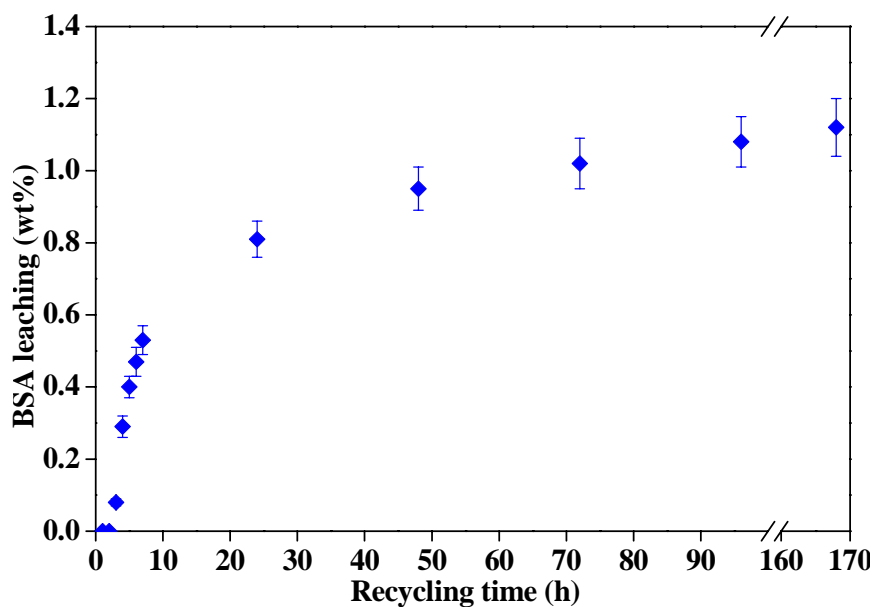


Figure 5 The amount of the BSA leached from the biofunctionalized nanofibers at different washing intervals (the onset time of the measurement is 1 h)

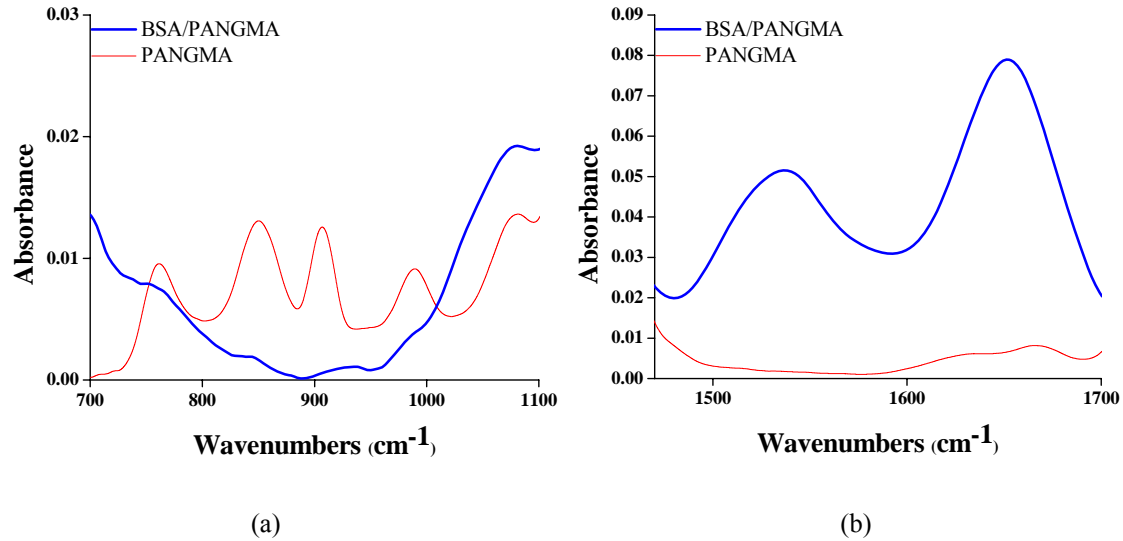


Figure 6 ATR-FTIR graphs showing : a) disappearance of the epoxy group and b) emergence of the amide groups upon the biofunctionalization

**Pore size and porosity measurement.** A concern always being felt with protein biofunctionalization of the nanofibrous membranes is their pore clogging and porosity loss. Such problems could consequently lead to a higher pressure drop and loss of permeability during filtration.

As seen in Figure 7, the porosity of the PANGMA ENM does not change significantly and remains constant after the biofunctionalization. However, the pore size declines. The reason for a smaller pore size could be sought in the growth of nanofibers present at the outermost layers through biofunctionalization via adsorption of protein ligands. In fact, it is assumed that the outermost layers are more exposed to protein and more functionalized rather than the internal nanofibers. Thus, a bottle-neck effect occurs during the pore size measurement which is frequently observed for the bubble point test.<sup>16</sup> Despite the pore size change, it still lies in the range of microfiltration.<sup>17</sup>



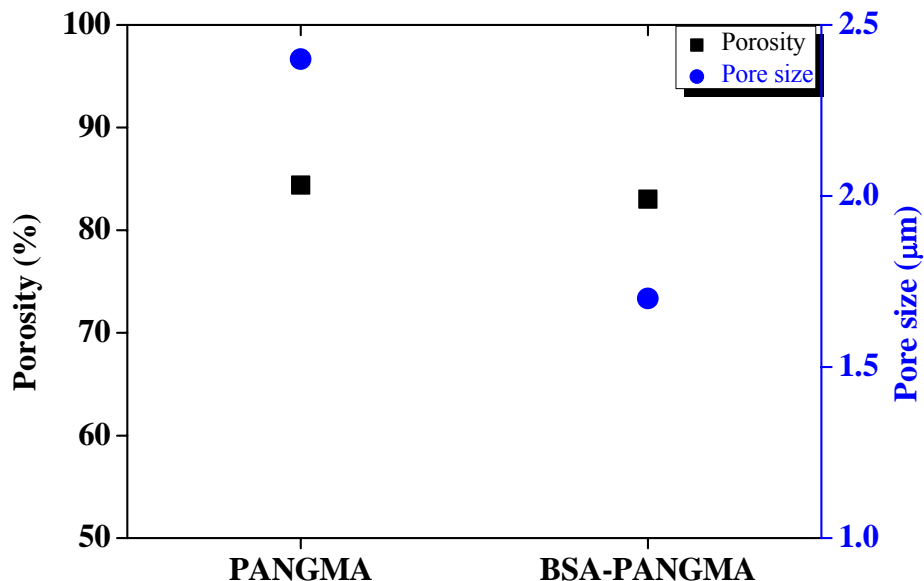


Figure 7 Porosity and pore size of the neat and biofunctionalized PANGMA ENMs

### **Wettability and Water uptake measurement of the BSA/PANGMA**

**nanofibrous membrane.** Wettability of a membrane is directly proportional to its filtration resistance. Electrospun nanofibrous membranes are normally made of hydrophobic materials due to their chemical and mechanical resistance.<sup>18</sup> The type of the membrane material used coupled with a highly nanorough structure leads to an ultrahydrophobicity in this kind of membranes. A hydrophobic membrane possesses a significant fouling tendency<sup>19</sup> and filtration resistance thereby giving rise to an extra pressure drop to fulfill the filtration progress i.e. an additional energy consumption and naturally cost.

In our study, water contact angle measurements (Figure 8) confirmed that the membranes after the biofunctionalization acquire an almost superhydrophilicity effect. This effect is mainly caused by the presence of the protein on the surface of the

nanofibers. Proteins are composed of amino acid monomers containing functional groups of amine and carboxyl.<sup>20</sup> This high functionality especially at wet state where due to a conformational change the functional groups are more exposed could lead to a higher interaction with water molecules thereby to induce a superhydrophilicity effect.<sup>9</sup>

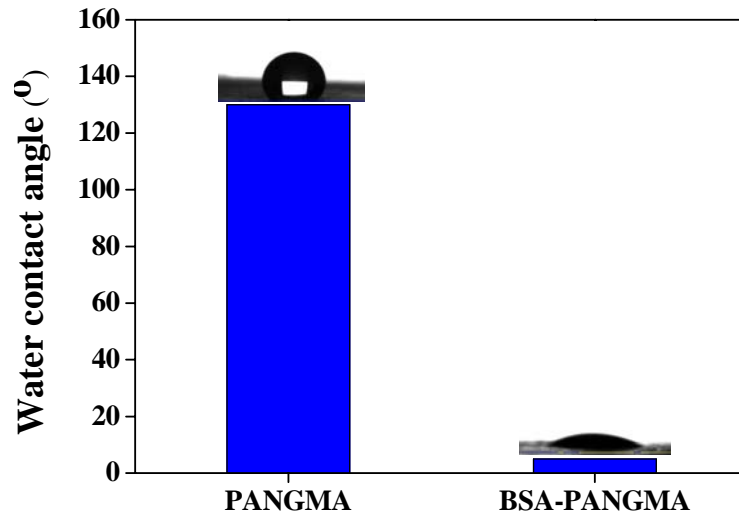


Figure 8 Wettability of the PANGMA ENMs before and after the biofunctionalization

To benefit the biofunctionalized membranes for some sort of non-pressure driven separations i.e. static adsorption based separations, water uptake of the membranes could be of importance. As observed in Figure 9, a water uptake test based on immersion of the samples in a water bath for 80 h, indicates a bimodal behaviour for the membranes as ascending and steady trends, respectively. At the primary stage, both the neat and biofunctionalized membranes show an ascending trend in term of water uptake with a higher rate for the latter membranes. Afterwards, both the membranes reach to a saturation state. While for the neat ENM it takes 4 h to become saturated, for the biofunctionalized one this duration does not exceed more than 1 h. As proved via the

water contact angle measurement, this difference in performance of the membranes could be attributed to a higher interaction between water molecules and the protein ligands present at the surface of the nanofibers.

Throughout the measurements, the biofunctionalized ENM always shows a higher water uptake capacity owing to the higher tendency of water molecules to the biofunctionalized nanofibers and their penetration into the biofunctionalized membrane.

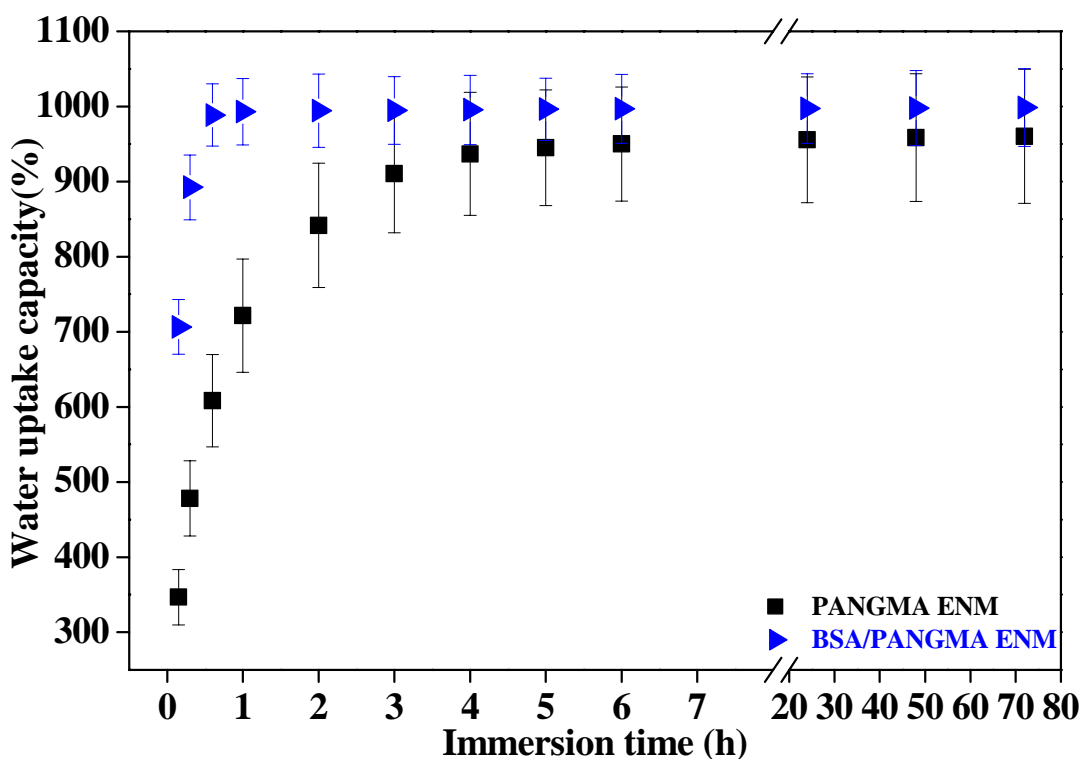


Figure 9 Water uptake behaviour of the neat and biofunctionalized PANGMA ENMs

**Thermal properties of the BSA/PANGMA nanofibrous membranes.** To investigate the influence of the biofunctionalization on thermal properties of the nanofibrous membranes, thermal glass transition temperature ( $T_g$ ) and thermal

decomposition temperature ( $T_d$ ) i.e. thermal stability of the PANGMA nanofibers before and after biofunctionalization were compared.

Figure 10 exhibits that the biofunctionalized membranes possess a higher level of thermal resistance. The main reason could be cross linking of the PANGMA chains stimulated by the functionalization process. The cross linking restricts local chain mobility thereby increases glass transition temperature.<sup>21</sup> Moreover, a higher thermal stability is induced by the cross linking<sup>22</sup> implying the feasibility of application of the biofunctionalized membrane at higher temperatures than ambient temperature.

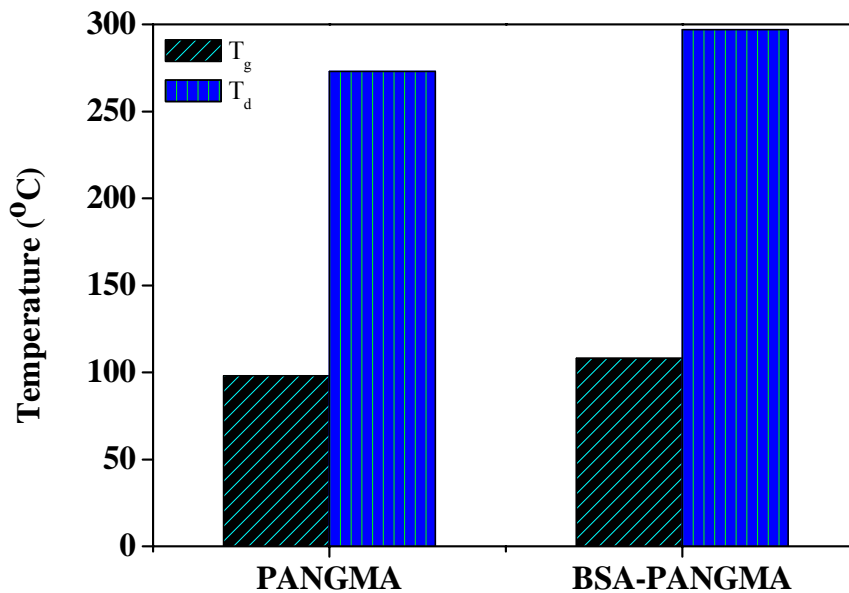


Figure 10 Variation of thermal properties of the PANGMA ENMs before and after the biofunctionalization

### **Mechanical properties of the BSA/PANGMA nanofibrous membranes.**

Despite promising filtration features, an electrospun membrane which is exposed to various stresses applied by fluid flow should also possess sufficient mechanical strength.<sup>23</sup> Without mechanical stability, the membrane undergoes mechanical failures

such as compaction which affects the filtration efficiency. Hence, mechanical strengthening of the electrospun nanofibrous membranes could be a very critical objective to broaden the range of their applications.<sup>24</sup>

As a prerequisite for pressure-driven liquid filtration applications, as seen in Figure 11, the biofunctionalization of the PANGMA ENMs could lead to a more optimum mechanical performance in terms of stiffness (elastic modulus) also strength. BSA ligands can concurrently bond to two adjacent nanofibers thereby form a physical cross linking (as shown in <sup>9</sup>). Such a network structure restricts movement of the nanofibers tending to pass by each other thereby optimizes the mechanical performance of the biofunctionalized membrane.

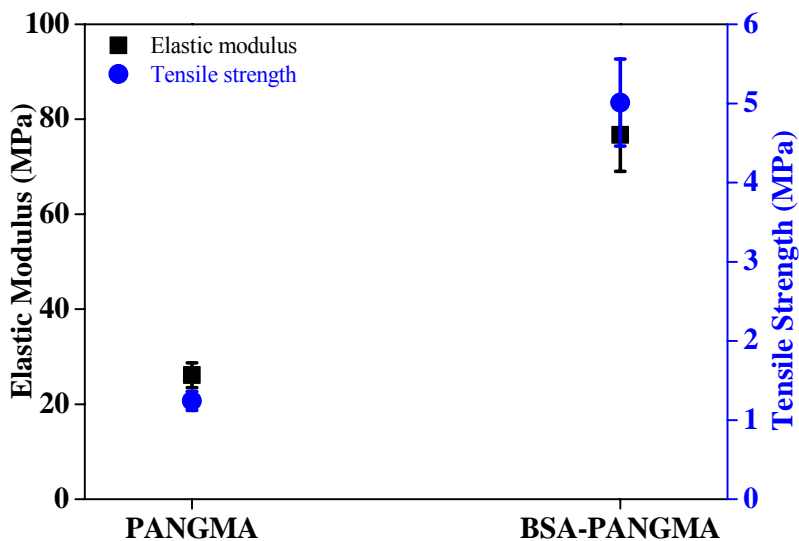


Figure 11 Tensile properties of the PANGMA ENMs before and after the biofunctionalization

**Water flux measurements.** A combination of superhydrophilicity and mechanical stability can bring about a much less filtration resistance to the water stream to be filtered i.e. a higher permeability.

As observed in Figure 12, a water flux measurement under a 1 bar feed pressure could readily prove that the membranes after biofunctionalization are more permeable i.e. possess a higher water flux. Considering almost equal porosity of the neat and biofunctionalized membranes, this high permeability as mentioned above is attributed to superhydrophilicity and strength of these membranes.<sup>15, 24</sup>

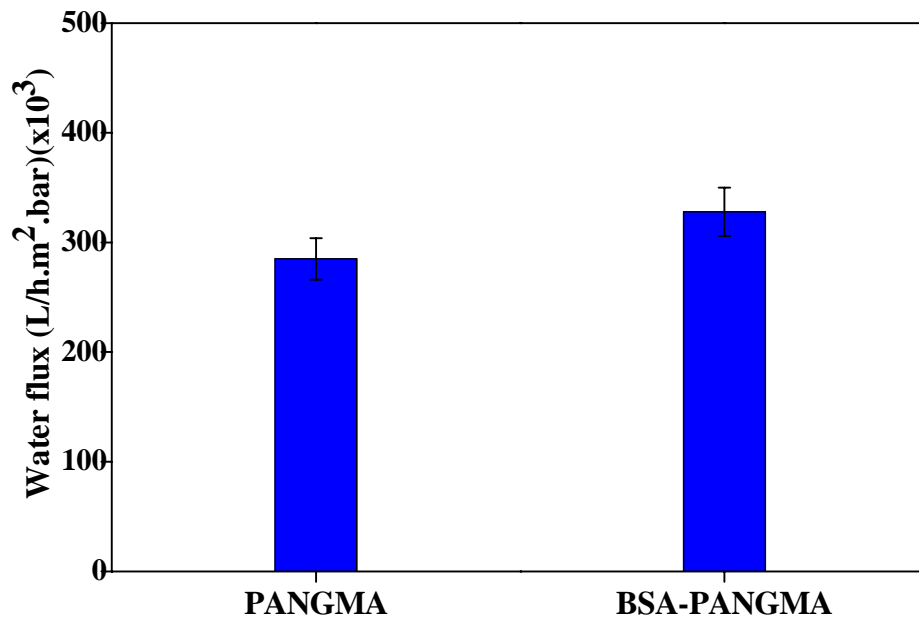


Figure 12 Water flux behaviour of the PANGMA ENMs before and after the biofunctionalization

**Protein filtration experiments.** One protein and an enzyme were selected to investigate adsorption ability i.e. selectivity of the BSA/PANGMA ENMs for organics and biomolecules. Considering the low price of BSA and its molecular weight range close to that of proteins and enzymes, it was selected as a protein model.<sup>25</sup> Cal-B is an enzyme chosen due to its catalytic activity useful for further applications i.e. as a heterogeneous catalysis. In case an efficient separation of Cal-B by the biofunctionalized ENM, the membrane can be subsequently used for catalysis applications.

The retention test results as shown in Figure 13 imply a high separation efficiency of the biofunctionalized ENMs compared to that of the neat ones. The adsorption of both BSA and Cal-B to the PANGMA ENM is as low as 8% confirming the suitability of the membrane to perform as an ideal affinity membrane.<sup>25</sup> While, the biofunctionalized ENM shows a high separation efficiency for BSA (63%) and Cal-B (58%) from their corresponding aqueous solutions. After 5 cycles of filtration, this efficiency reaches to 88% and 81% for BSA and Cal-B, respectively. This filtration efficiency is a breakthrough when we consider the minor concentration of the protein solution which normally should pass through a macroporous structured membrane as ours. Also, filtration as dynamical minimizes the residence time of the protein on the nanofibers and the chance of its interaction and capturing by the membrane. Despite the challenges, the biofunctionalized ENM is successful in removal of the protein models.

Presence of a protein coat layer rich of functional groups especially in aqueous media could definitely lead to the highest level of functionality for the biofunctionalized ENM. The protein solutes i.e. BSA and Cal-B can readily interact with the BSA ligands immobilized onto the nanofibers thereby a high separation efficiency is acquired. During

a water treatment, the proteins whether those immobilized or as solutes undergo a conformational change. This change brings about emergence of the hidden functional groups in a protein folded. Upon the emergence, the functional groups being exposed can interact with their counterparts present on the protein to be separated and consequently give rise to a high separation efficiency. As we showed previously<sup>9</sup>, the conformational change and subsequent swelling of the biofunctional agent results in a large steric hindrance i.e. pore size decline as well thereby a contribution to the optimum separation efficiency. Figure 14 shows SEM images of the BSA protein separated by the biofunctionalized ENM.

On the whole, the BSA/PANGMA ENM could show an optimum ability in selective separation of proteins from water. While this task is normally done by ultrafiltration membranes at a feed pressure of several bars (1-5 bar) and with a low water permeability (50-200 L/h.m<sup>2</sup>)<sup>18</sup>, our biofunctionalized electrospun nanofibrous membranes possessing a high functional surface area can perform this task optimally under a very low applied feed pressure and with an extraordinary permeability i.e. cost efficiency.



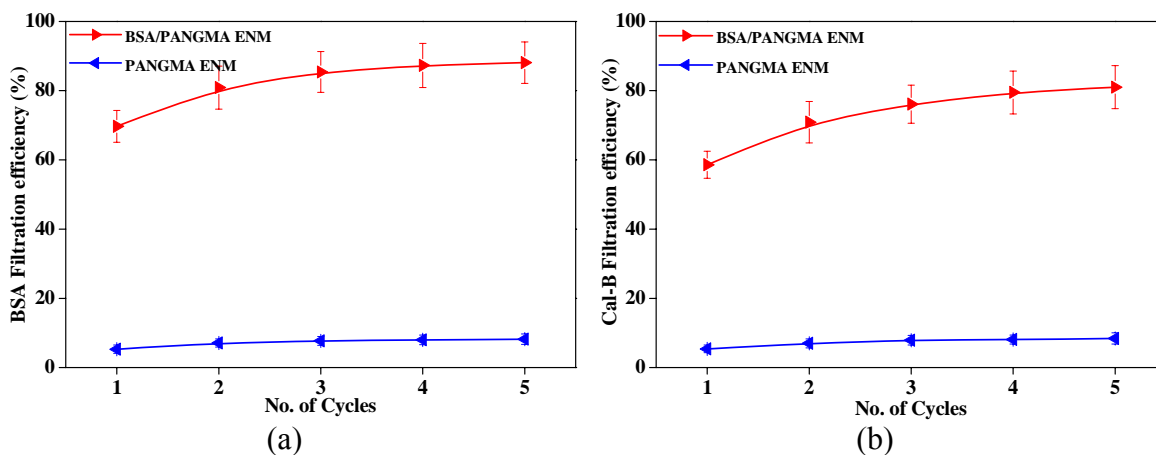


Figure 13 Protein retention efficiency of the PANGMA ENMs before and after the biofunctionalization

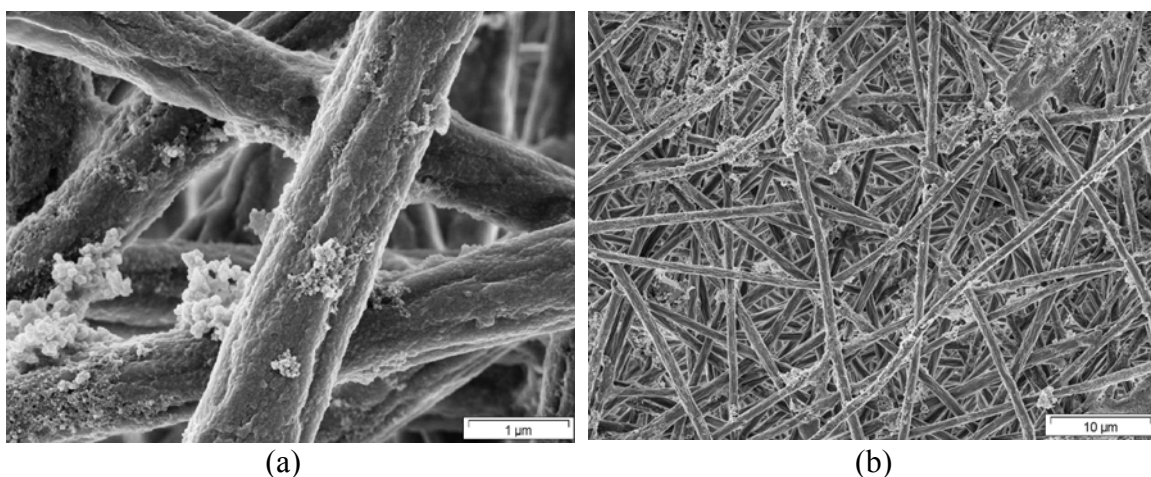


Figure 14 SEM micrographs showing separation of BSA protein by the BSA/PANGMA ENMs (a:20,000x, b:2000x)

## ■ Author information

**Corresponding author:**

\* E-mail: [mady.elbahri@hzg.de](mailto:mady.elbahri@hzg.de)

## ■ Acknowledgements

M. Elbahri thanks the initiative and networking fund of the Helmholtz Associations for providing the financial base of the start-up of his research group. The authors would like to acknowledge Kristian Bühr for design of water flux measurement

set-up, Joachim Koll for bubble point test, Silvio Neumann for TGA and DSC measurements, Heinrich Böttcher for tensile tests, and Karen-Marita Prause for SEM measurements.

## References

1. Ramakrishna, S.; Fujihara, K.; Teo, W.-E.; Yong, T.; Ma, Z.; Ramaseshan, R., Electrospun nanofibers: solving global issues. *Mater.Today* 2006, 9(3), 40-50.
2. Ma, Z. W.; Kotaki, M.; Ramakrishna, S., Electrospun cellulose nanofiber as affinity membrane. *J. Membr. Sci.* 2005, 265(1-2), 115-123.
3. Bamford, C. H.; Allamee, K. G.; Purbrick, M. D.; Wear, T. J., Studies of a Novel Membrane for Affinity Separations .1. Functionalization and Protein Coupling. *J. Chromatogr.* 1992, 606 (1), 19-31.
4. Ma, Z.; Kotaki, M.; Ramakrishna, S., Surface modified nonwoven polysulphone (PSU) fiber mesh by electrospinning: A novel affinity membrane. *J. Membr. Sci.* 2006, 272, 179-187.
5. Zhang, H.; Nie, H.; Yu, D.; Wu, C.; Zhang, Y.; White, C. J. B.; Zhu, L., Surface modification of electrospun polyacrylonitrile nanofiber towards developing an affinity membrane for bromelain adsorption. *Desalination* 2010, 256 (1-3), 141-147.
6. Lu, P.; Hsieh, Y.-L., Lipase bound cellulose nanofibrous membrane via Cibacron Blue F3GA affinity ligand. *J. Membr. Sci.* 2009, 330, (1-2), 288-296.
7. Ma, Z.; Masaya, K.; Ramakrishna, S., Immobilization of Cibacron blue F3GA on electrospun polysulphone ultra-fine fiber surfaces towards developing an affinity membrane for albumin adsorption. *J. Membr. Sci.* 2006, 282, 237-244.
8. Ma, Z.; Lan, Z.; Matsuura, T.; Ramakrishna, S., Electrospun polyethersulfone affinity membrane: Membrane preparation and performance evaluation. *J. Chromatogr. B-Anal. Technol. Biomed. Life Sci.* 2009, 877 (29), 3686-3694.
9. Elbahri, M.; Homaeigohar, Sh.; Dai, T.; Abdelaziz, R.; Khalil, R.; Zillohu, A. U., Smart Metal-Polymer Bionanocomposites as Omnidirectional Plasmonic Black Absorbers Formed by Nanofluid Filtration. *Adv. Funct. Mater.* In Press, 2012.
10. Godjevargova, T.; Konsulov, V.; Dimov, A., Preparation of an ultrafiltration membrane from the copolymer of acrylonitrile-glycidylmethacrylate utilized for immobilization of glucose oxidase. *J. Membr. Sci.* 1999, 152(2), 235-240.

11. Dai, T.; Miletic, N.; Loos, K.; Elbahri, M.; Abetz, V., Electrospinning of Poly[acrylonitrile-co-(glycidyl methacrylate)] Nanofibrous Mats for the Immobilization of Candida Antarctica Lipase B. *Macromol. Chem. Phys.* 2010, 212(4), 319-327.
12. Hicke, H. G.; Lehmann, I.; Malsch, G.; Ulbricht, M.; Becker, M., Preparation and characterization of a novel solvent-resistant and autoclavable polymer membrane. *J. Membr. Sci.* 2002, 198(2), 187-196.
13. Na, H.; Zhao, Y.; Liu, X.; Zhao, C.; Yuan, X., Structure and properties of electrospun poly(vinylidene fluoride)/polycarbonate membranes after hot press. *J. Appl. Polym. Sci.* 2011, 122, 774-781.
14. Homaeigohar, SSh.; Buhr, K.; Ebert, K., Polyethersulfone electrospun nanofibrous composite membrane for liquid filtration. *J. Membr. Sci.* 2010, 365, 68-77.
15. Homaeigohar, SSh.; Mahdavi, H.; Elbahri, M., Extraordinarily water permeable sol gel formed nanocomposite nanofibrous membranes. *J. Colloid Interface Sci.* 2012, 366, 51-56.
16. Nisbet, DR.; Rodda, AE.; Finkelstein, DI.; Horne, MK.; Forsythe, JS.; Shen, W., Surface and bulk characterisation of electrospun membranes: Problems and improvements. *Coll. Surf. B: Biointerfaces* 2009, 71, 1-12.
17. Mulder, M., *Basic Principles of Membrane Technology*. Kluwer Academic: Boston, 1996.
18. Ramakrishna, S.; Jose, R.; Archana, P. S.; Nair, A. S.; Balamurugan, R.; Venugopal, J.; Teo, W. E., Science and engineering of electrospun nanofibers for advances in clean energy, water filtration, and regenerative medicine. *J. Mater.Sci.* 2010, 45, (23), 6283-6312.
19. Baker, R., *Membrane technology and applications*. 2nd edition ed.; Wiley: 2004.
20. Stevens, M., *Polymer Chemistry; An Introduction*. OXFORD UNIVERSITY PRESS: Oxford, 1999.
21. Krumova, M.; Lopez, D.; Benavente, R.; Mijangos, C.; Perena, J. M., Effect of crosslinking on the mechanical and thermal properties of poly(vinyl alcohol). *Polymer* 2000, 41, (26), 9265-9272.
22. Marechal, E., Chemical modification of synthetic polymers. In *Comprehensive polymer science*, GC Eastmond; A Ledwith; S Russo; Sigwalt, P., Eds. Pergamon: Oxford, 1989; Vol. 6, pp 1-47.
23. Yoon, K.; Hsiao, BS.; Chu, B., Formation of functional polyethersulfone electrospun membrane for water purification by mixed solvent and oxidation processes. *Polymer* 2009, 50(13), 2893-2899.
24. Homaeigohar, SSh.; Elbahri, M., Novel compaction resistant and ductile nanocomposite nanofibrous microfiltration membranes. *J. Colloid Interface Sci.* 2012, 372, 6-15.
25. Zhu, J.; Yang, J.; Sun, G., Cibacron Blue F3GA functionalized poly(vinyl alcohol-co-ethylene) (PVA-co-PE) nanofibrous membranes as high efficient affinity adsorption materials. *J. Membr. Sci.* 2011, 385 (1-2), 269-276.

# TOC Figure

